

Supporting Information for manuscript entitled

A New Strategy to Enhance Phosphate Removal from Water by Hydrous Manganese Oxide

Bingcai Pan*, Feichao Han, Guangze Nie, Bing Wu, Kai He, Lv Lu

State Key Laboratory of Pollution Control and Resource Reuse, School of the
Environment, Nanjing University, Nanjing 210023, PR China

The *Supporting Information Available* contains 14 pages, including
Scheme S1, Figures S1-S7, and Tables S1-S4.

Scheme S1 The historic relationship between three polymeric hosts.

Figure S1 The particle size distribution nano-HMO inside NS with the aid of Nano
Measure (Version 1.2, ZKBC)

Figure S2 XPS spectra of manganese species in HMO@NS and HMO.

Figure S3 Zeta potentials of HMO and HMO@NS at different pH values.

Figure S4 Potentiometric titration curves of CS and NS as compared to water

Figure S5 TEM images of three polymer-based HMO nanocomposite and the bulky
one. (a) HMO@NS; (b) HMO@SS; (c) HMO@CS; (d) HMO.

Figure S6 Phosphate adsorption kinetics by NS and HMO@NS at 298 K and pH 7.0.
Each adsorbent dose was 0.5 g/L. Initial phosphate was 10 mg P/L.

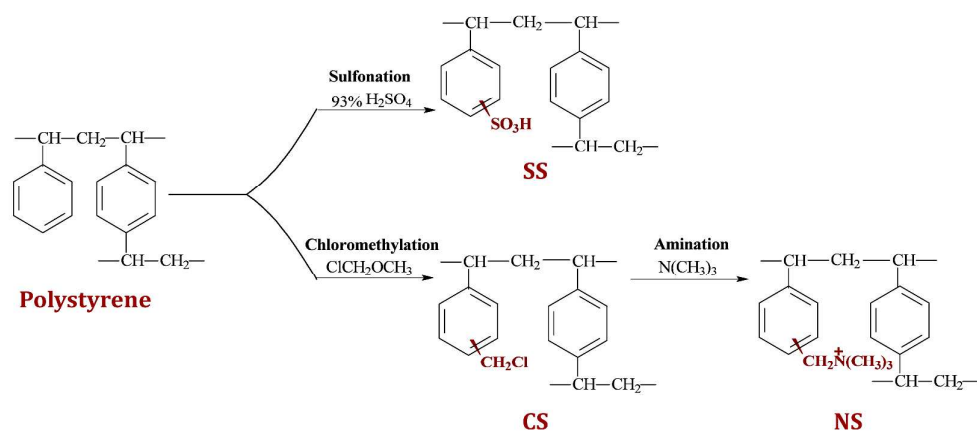
Figure S7 Adsorption isotherms of HMO@NS and NS at 298 K, pH 7.0. Each
adsorbent dose was 0.5 g/L.

Table S1 The intraparticle diffusion model parameters for phosphate adsorption on
HMO@NS and NS.

Table S2 Langmuir and Freundlich model parameters for phosphate adsorption on
HMO@NS and NS

Table S3 Comparison of adsorption capacity of different phosphate adsorbents

Table S4 Basic properties of the real effluent from a WWTP in Nanjing city



Scheme S1 The historic relationship between three polymeric hosts

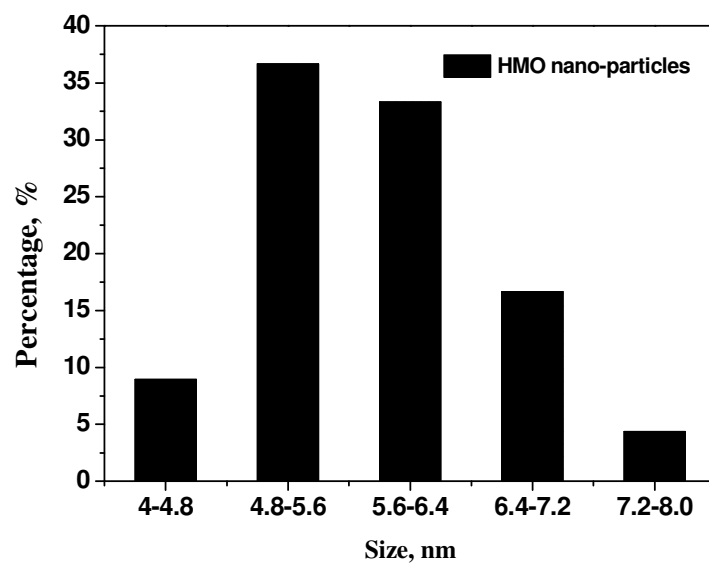


Figure S1 Particle size distribution of nano-HMO inside NS with the aid of Nano Measure (Version 1.2, ZKBC)

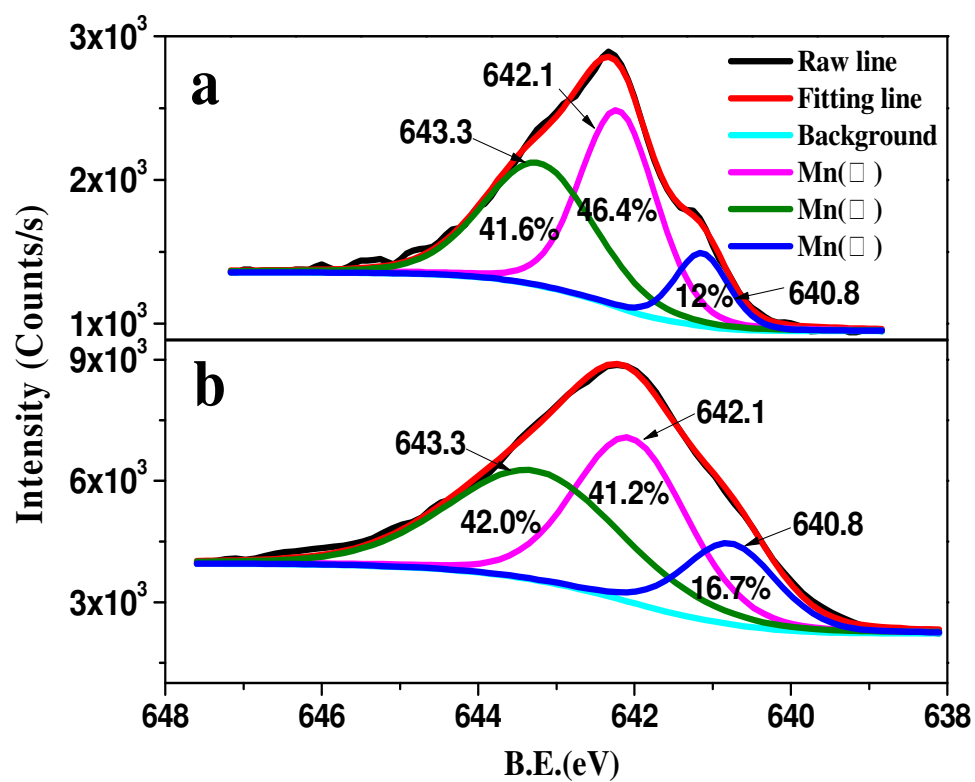


Figure S2 XPS spectra of manganese species in HMO@NS and HMO (a) HMO@NS; (b) HMO

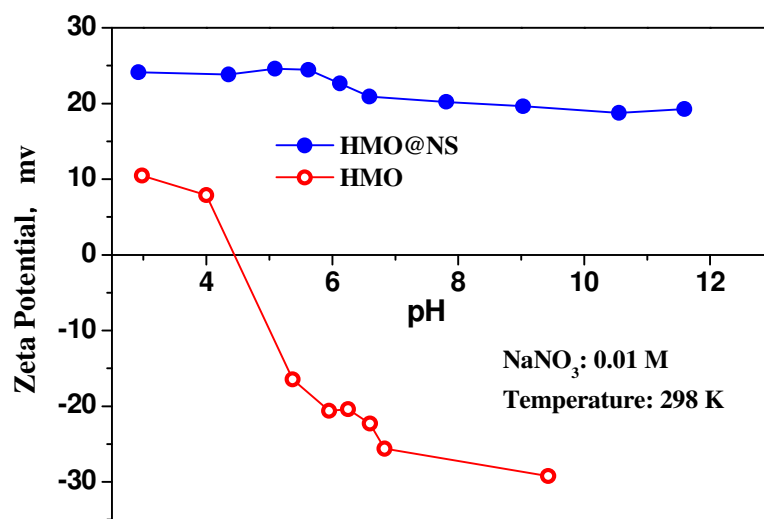


Figure S3 Zeta potentials of HMO and HMO@NS at different pH values.

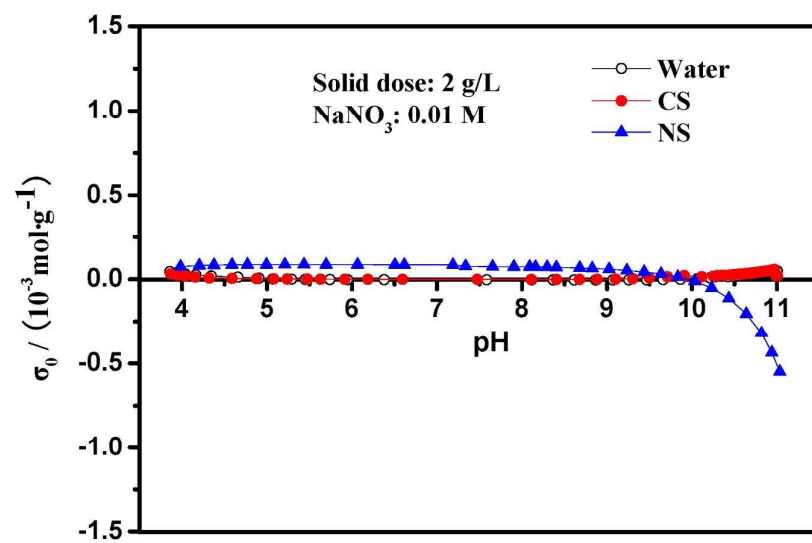


Figure S4 Potentiometric titration curves of CS and NS as compared to water

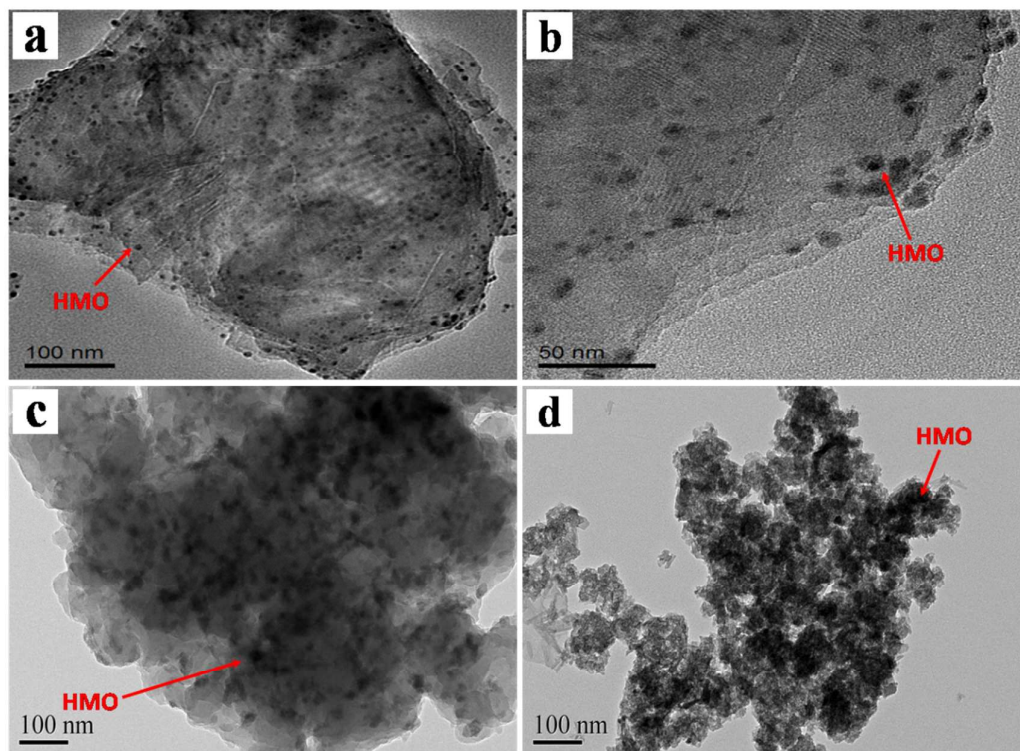


Figure S5 TEM images of three polymer-based HMO nanocomposites and the bulky one. (a) HMO@NS; (b) HMO@SS; (c) HMO@CS; (d) HMO

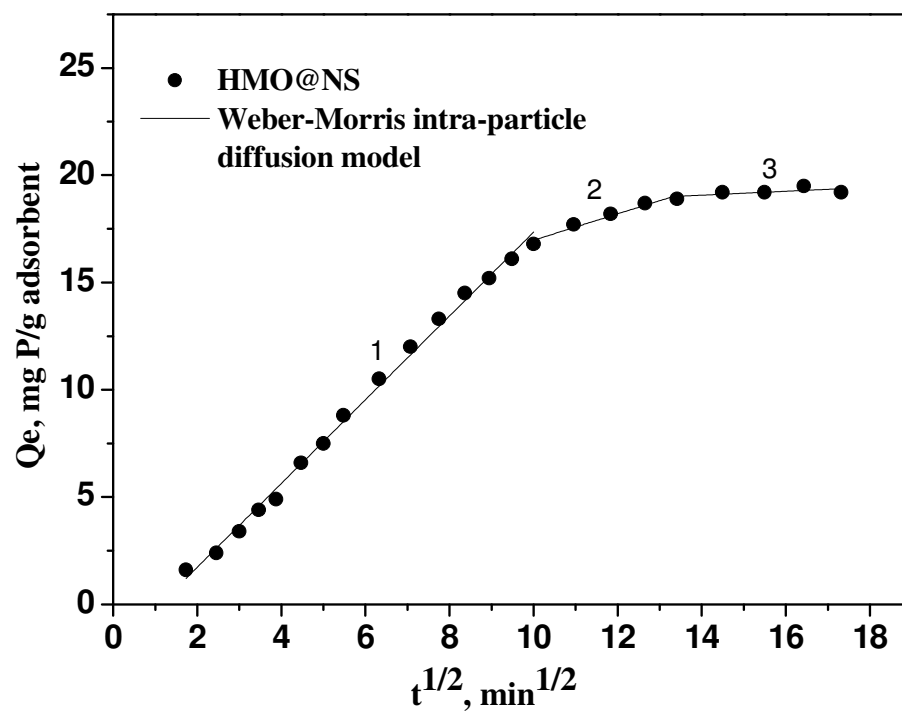


Figure S6 Phosphate adsorption kinetics from the background by HMO@NS at 298 K and pH 7.0. Adsorbent dose was 0.5 g/L. Initial phosphate was 10 mg P/L.

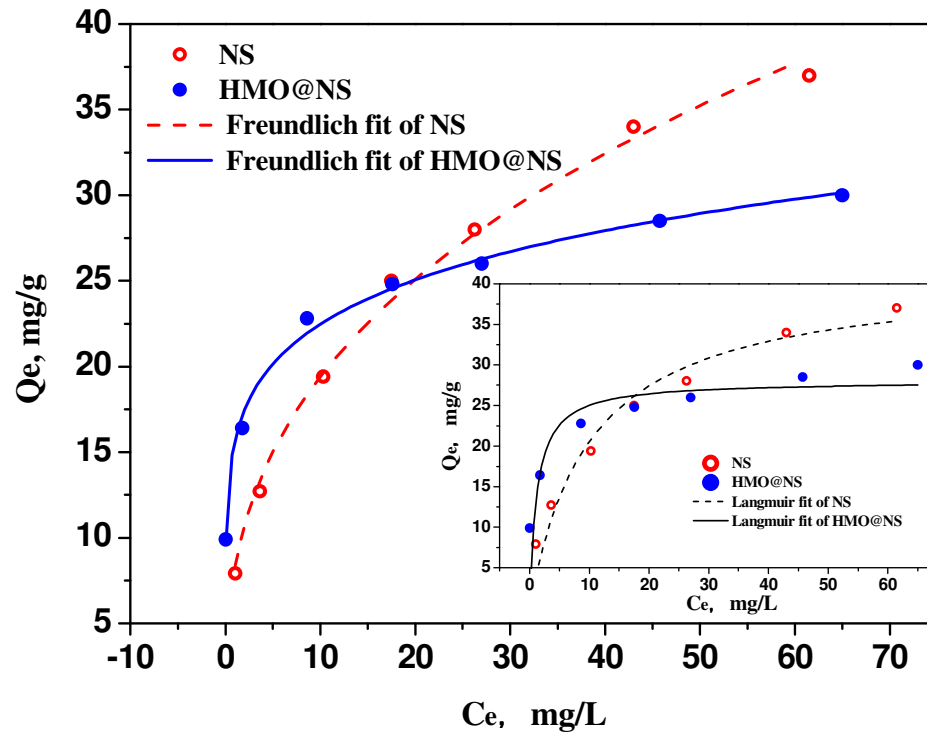


Figure S7 Adsorption isotherms of HMO@NS and NS at 298 K, pH 7.0. Each adsorbent dose was 0.50 g/L.

Table S1

The intraparticle diffusion model parameters for phosphate adsorption on HMO@NS and NS

Adsorbent	Intraparticle diffusion model					
	K_{p1}	I	R^2	K_{p2}	I	R^2
HMO@NS	1.64	0	0.993	0.502	12.2	0.966
NS	1.26	0	0.991			

K_{p1} : Intraparticle diffusion rate constant of the first step for HMO@NS or NS;

K_{p2} : Intraparticle diffusion rate constant of the second step for HMO@NS;

I : Y -intercept.

Table S2

Langmuir and Freundlich model parameters for phosphate adsorption on NS and HMO@NS.

Adsorbent	Langmuir model			Freundlich model		
	$q_{max}(\text{mg/g})$	$b(\text{L/mg})$	R^2	$K_{[\text{mg/g} \cdot (\text{L/g})^n]}$	n	R^2
NS	41.2	0.099	0.950	8.25	2.69	0.994
HMO@NS	28.0	0.833	0.644	15.66	6.37	0.994

Table S3

Comparison of adsorption capacity of different phosphate adsorbents

Adsorbents	q_{\max}	References
Fly ash	20.2	1
Blast furnace slag	18.9	2
CMOMO	26.3	3
Ferric sludge	25.5	4
Acid mine drainage sludge	32.0	5
Iron oxide tailings	8.2	6
Aluminum	23.0	7
Fe oxide tailing	21.5	8
Fe(III)/Cr(III) hydroxide	6.5	9
Fe-Mn binary oxide adsorbent	36	10
MgMn-layered double hydroxides	22.3	11
HMO@NS	>29.78*	Present study

* Obtained from the Freundlich adsorption isotherm (Figure S7 and Table S2) at the equilibrium concentration of 60 mg P/L.

Table S4

Basic properties of the real effluent sampled from a WWTP in Nanjing city.

pH	Phosphate (mg P/L)	Cl ⁻ (mg/L)	SO ₄ ²⁻ (mg/L)	NO ₃ ⁻ (mg/L)	Mg ²⁺ (mg/L)	Ca ²⁺ (mg/L)	NH ₄ ⁺ -N (mg/L)	COD (mg/L)
7.2	1.3	71.3	47.5	26.4	11.3	67.6	0.5	18.7

Literature cited

1. Chen, J.; Kong, H.; Wu, D.; Chen, X.; Zhang, D.; Sun, Z., Phosphate immobilization from aqueous solution by fly ashes in relation to their composition. *J. Hazard. Mater.* 2007, 139 (2), 293-300.
2. Kostura, B.; Kulveitova, H.; Leško, J., Blast furnace slags as sorbents of phosphate from water solutions. *Water Res.* 2005, 39 (9), 1795-1802.
3. Liu, T.; Wu, K.; Zeng, L., Removal of phosphorus by a composite metal oxide adsorbent derived from manganese ore tailings. *J. Hazard. Mater.* 2012, 217, 29-35.
4. Song, X.; Pan, Y.; Wu, Q.; Cheng, Z.; Ma, W., Phosphate removal from aqueous solutions by adsorption using ferric sludge. *Desalination.* 2011, 280 (1), 384-390.
5. Wei, X.; Viadero Jr., R. C.; Bhojappa, S. Phosphorus removal by acid mine drainage sludge from secondary effluents of municipal wastewater treatment plants, *Water Res.* 2008, 42 (13) , 3275-3284.
6. L. Zeng, X. Li, J. Liu, Adsorptive removal of phosphate from aqueous solutions using iron oxide tailings, *Water Res.* 2004, 38, (5), 1318–1326.
7. Babatunde, A. O.; Zhao, Y.; Burke, A. M.; Morris, M. A.; Hanrahan, J. P. Characterization of aluminium-based water treatment residual for potential phosphorus removal in engineered wetlands, *Environ. Pollut.* 2009, 157, 2830-2836.
8. Zeng, L.; Li, X.; Liu, J. Adsorptive removal of phosphate from aqueous solutions using iron oxide tailings. *Water Res.* 2004, 38(5), 1318-1326.
9. Namasivayam, C.; Prathap, K., Recycling Fe(III)/Cr(III) hydroxide, an industrial solid waste for the removal of phosphate from water. *J. Hazard. Mater.* 2005, 123 (1-3), 127–134.
10. Zhang, G.; Liu, H.; Liu, R.; Qu, J., Removal of phosphate from water by a Fe-Mn binary oxide adsorbent. *J. Colloid Interface Sci.* 2009, 335 (2), 168-174.
11. Chitrakar, R.; Tezuka, S.; Sonoda, A.; Sakane, K.; Ooi, K.; Hirotsu, T., Adsorption of phosphate from seawater on calcined MgMn-layered double hydroxides. *J. Colloid Interface Sci.* 2005, 290(1), 45-51.